Catalysis Science & Technology

Accepted Manuscript

ROYAL SOCIETY OF CHEMISTRY

www.rsc.org/catalysis

Journal Name

RSCPublishing

Minireview

Interactions between metal species and nitrogen-functionalized carbon nanotubes

Cite this: DOI: 10.1039/x0xx00000x

Wei Xia

Received 00th January 2012,
Accepted 00th January 2012

DOI: 10.1039/x0xx00000x

www.rsc.org/

Nitrogen-functionalized carbon nanotubes are promising materials in catalysis due to their versatile surface properties involving nitrogen groups, oxygen groups, surface defects and metal impurities. These factors can be used to tune the dispersion, morphology, crystal structure, electronic structure, mobility/stability and finally the catalytic performance of supported metal nanoparticles. This review focuses on selected examples aiming at understanding the interactions between surface groups, defects, and metal species and their impact on the catalytic properties in electrocatalysis and gas-phase redox catalysis.

1. Introduction

Carbon nanotubes (CNTs) are promising materials for various applications due to their unique structural and electronic properties. After more than 20 years of intensive research and development, the industrial production of CNTs has been established mainly using catalytic chemical vapor deposition in fluidized-bed reactors.[1, 2] While the production of CNTs is no longer a technical problem, their large-scale industrial application remains challenging.[3, 4] Further fundamental understanding and technical development are essentially needed for the commercialization of CNTs, for example, as functional materials in catalysis.[5-8] The incorporation of nitrogen atoms in CNTs considerably broadens their potential applications due to favourably modified surface and bulk properties.[9, 10] Among others, catalysis is one of the most promising fields for the application of nitrogen-doped or nitrogen-functionalized CNTs (NCNTs).[11, 12] On the one hand, NCNTs are intrinsically active for various reactions including electrocatalytic oxygen redox reactions[13-15] and gas-phase catalytic reactions such as H_2S oxidation and olefin hydrogenation reactions.[16-20] On the other hand, NCNTs are unique support materials for catalysts both for gas-phase and liquid-phase reactions.[21-24]

Both "nitrogen-doped" and "nitrogen-functionalized" CNTs are used to describe CNTs with nitrogen species incorporated in the bulk and/or on the surface. Generally, doping refers more to the bulk and functionalization more to the surface. Typically, NCNTs synthesized by catalytic growth using nitrogen-containing precursors contain nitrogen both in the bulk and on the surface,[25-31] while those obtained by post-treatment of CNTs using nitrogen-containing precursors like ammonia, contain nitrogen mainly on the surface.[32, 33] As to post-treatment using nitrogen-containing hydrocarbons or coating of nitrogen-containing polymers, nitrogen species can be found in the surface layers of those NCNTs.[34] Nevertheless, it is often difficult to depict the exact location of nitrogen due to limited characterization methods and the presence of a large amount of defects in NCNTs.[35]

In addition to nitrogen, even NCNTs synthesized by catalytic growth always contain a considerable amount of oxygen.[36] This is rather confusing when taking into account the typical growth conditions: nitrogen-containing carbon source together with hydrogen at high temperature followed by cooling in inert gas.[37] However, it is conceivable that oxygen may originate from the metal oxide used as growth catalyst, from impurities/leakage or even upon contact with air after cooling. In other words, oxygen cannot be fully excluded when performing the synthesis under ambient conditions. Nearly all the studies involving NCNTs in catalysis, regardless of their exact role therein – as support materials or as active phase – focus on the nitrogen species on the NCNT surface, while the oxygen species on NCNTs were seldom investigated or discussed.[38, 39]

In addition to oxygen and nitrogen, metal species are often involved in the catalytic application of NCNTs.[40] On the one hand, the catalytic synthesis of CNTs or NCNTs needs metal catalysts, which cannot be completely removed prior to applications.[37, 41] On the other hand, metal and/or metal oxide nanoparticles can be deposited on NCNTs used as support in catalysis.[24] In both cases, metal species can be influenced by nitrogen and oxygen species on the NCNT surface. Furthermore, the incorporation of both oxygen and nitrogen atoms introduces defects in carbon materials.[35] Among others, disordered or amorphous carbon, point defects in graphene sheets, edge planes and surface carbon layers or debris can be created or removed by oxidation treatment.[42] These defects show chemical and physical properties different from graphitic CNTs and therefore often play an important role in the catalytic application of NCNTs. Defects may also be present in metal or metal oxide nanoparticles deposited on NCNTs depending on the applied redox conditions.[43, 44] Carbide or nitride may form at the interface between the nanoparticles and the NCNT support after thermal treatment during sample preparation.[45, 46]

As a whole, the metal-NCNT system is schematically illustrated in Fig. 1. The interaction between metal and NCNTs can be influenced by a number of factors including nitrogen and oxygen species in NCNTs, defects on NCNTs, surface oxide in case of metal particles, oxygen deficiency and nitrogen doping in case of oxide particles. Additionally, another oxide can be deposited, which may have significant influence on the metal-support interactions. These factors can be used to tune the dispersion, morphology, crystal structure, electronic structure, mobility/stability and finally the catalytic performance of the supported particles. Also physical properties like conductivity and hydrophilicity/hydrophobicity, which play essential roles in electrocatalysis in the liquid phase, can be adjusted by these factors.

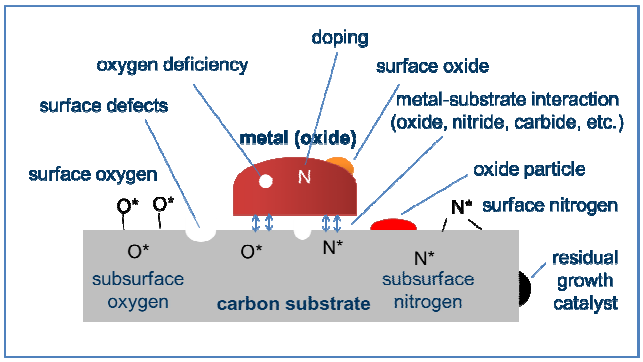

Fig. 1. Schematic illustration of the metal/NCNT system.

2. Essential differences between oxygen and nitrogen groups on carbon

Both the oxygen- and nitrogen-containing groups can act as anchoring points for foreign species, for example, metal precursors. Both of them can improve the hydrophilicity and the wetting properties of CNTs. However, there are significant differences between these two heteroatoms in carbon materials:

(1) In general, oxygen species are functional groups anchored on the carbon surface, although the embedding of oxygen in the graphitic structure is possible, for example, forming ether bonds at defect sites or even between neighbouring layers at edge sites.[47] In contrast, nitrogen species can be more easily incorporated in the graphitic structure of carbon, for example, as quaternary nitrogen in the basal plane or as pyridinic group at edge sites. This difference lies on the bonding properties of the two atoms. Nitrogen can be bonded with three carbon atoms, while oxygen can only be bonded with two. Obviously, nitrogen is more compatible to the sp^2 carbon network, whereas oxygen atoms can hardly be incorporated into the carbon network without bulk defects.

(2) Related to this chemical bonding, nitrogen tends to create surface or bulk defects in the graphitic carbon structure, while oxygen is more commonly anchored by grafting on the surface. Therefore, the type and amount of defects on/in OCNTs and NCNTs are different.

(3) Their thermal stability in inert gas is very different as nitrogen species are far more stable than oxygen species. The decomposition of anchored oxygen groups starts from about 200 °C, whereas nitrogen species remain stable at about 600 °C or even higher temperatures in inert atmosphere. Under air, NCNTs are less stable than OCNTs due to typically more disordered structure of NCNTs.

(4) Although both of them increase the hydrophilicity of carbon surface, oxygen groups interact more strongly with H_2O molecules;

(5) Oxygen and nitrogen have a different influence on the electronic structure of carbon materials. While both cause the loss of electronic conductivity when comparing with pure graphite, nitrogen has a much less negative influence on conductivity or charge transfer.

(6) OCNTs and NCNTs show different surface acidities. Oxygen groups are typically more acidic while nitrogen groups are more basic. The surface acidity can be modified by thermal treatment, which removes certain groups from the surface.

These differences between oxygen and nitrogen species on CNTs are not individual phenomena but correlated. The form of chemical bonding determines the defect level, and subsequently the thermal stability, electron transport, and interaction with foreign molecules or hydrophilicity. Detailed discussion and experimental evidence will be provided in the following sections.

3. Interaction between O, N and defects on carbon surface

3.1 Formation of surface oxygen and nitrogen

Oxygen- and nitrogen-containing functional groups on the surface of CNTs have been intensively studied in recent years. Oxygen functionalization can be achieved by partial oxidation, which is typically performed by refluxing in concentrated HNO_3.[47-49] Early studies disclosed the formation of carboxylic acid, anhydride, lactone, phenolic hydroxyl, carbonyl, and quinone groups after oxidation treatment.[50] Upon heating these groups decompose and release from carbon surface in form of CO and CO_2.[50-52] Typically, oxidized carbon shows acidic surface properties, which can be especially assigned to CO_2-releasing groups.[50, 53] We have developed a simple and highly effective gas-phase method for the functionalization of CNTs with HNO_3 vapor, thus eliminating separation by filtration.[54] A significantly higher amount of oxygen species compared with conventional wet HNO_3 treatment was achieved, and the morphology and the degree of agglomeration did not deteriorate because of the treatment.[54] Another major advantage of this gas-phase method is temperature variation. Temperature plays an important role in partial oxidation reactions on carbon surfaces. It was found that nitric acid oxidation at high temperatures like 200 °C favored the formation of C=O groups, whereas oxidation at low temperatures like 125 °C resulted in more C-O species.[54] In addition to temperature, treatment time also influences the formation of surface oxygen groups. X-ray photoelectron spectroscopy (XPS) is the most powerful method to investigate the chemical surface composition of CNTs. Fig. 2 shows the normalized O 1s XP core level spectra of the OCNT samples obtained by nitric acid vapor treatment at different temperatures for different durations. The two major contributions can be assigned to oxygen doubly bound to carbon (C=O) in quinones, ketones, and aldehydes at 531.6 eV and oxygen singly bound to carbon (i.e., O−C) in ethers, hydroxyls, and phenols at 533.2 eV. It can be seen that the total amount of oxygen indicated by the peak area increased with increasing treatment time from 24 to 72 h and decreased with further increase to 120 h. As to temperature variation, the amount of total oxygen remained unchanged with increasing temperature from 200 to 225 °C and decreased significantly with a further increase of treatment temperature to 250 °C. The low oxygen content at high temperatures is related to the limited thermal stability of the surface oxygen groups, especially of the carboxyl groups.

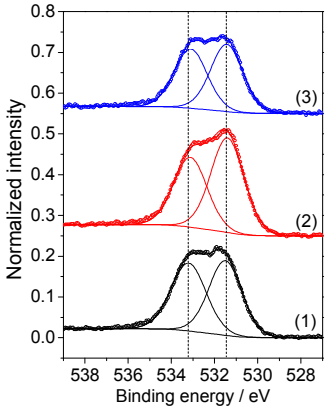

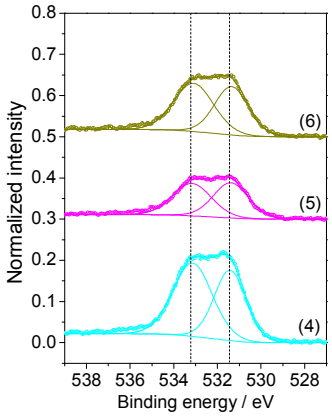

Fig. 2. XP O 1s spectra of OCNTs obtained by HNO_3 vapor treatment of purified CNTs at different temperature for different treatment durations. The spectra were normalized to the intensity of the corresponding C 1s spectra. (1) 200 °C, 24 h; (2) 200 °C, 72 h; (3) 200 °C, 120 h; (4) 225 °C, 24 h; (5) 250 °C, 24 h; (6) 250 °C, 12 h. Adapted from reference.[36]

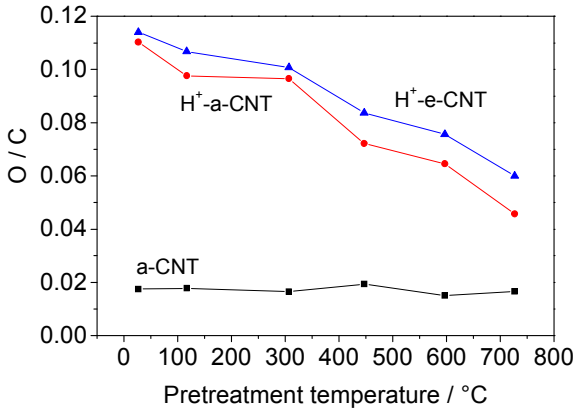

Fig. 3. Oxygen to carbon ratio (O/C) as a function of pretreatment temperature of as-is CNTs (a-CNT), HNO_3-treated as-is CNTs (H^+-a-CNT) and HNO_3-treated etched CNTs (H^+-e-CNT). The O to C ratios were derived from XPS surface atomic concentrations. The thermal treatments were carried out in the UHV chamber of the XPS setup. Adapted from reference.[59]

Nitrogen can be incorporated into CNTs either by feeding nitrogen-containing precursors during the CNT synthesis, or by the post-treatment of CNTs with nitrogen-containing molecules.[34, 37, 55] Different nitrogen-containing species can be incorporated in CNTs including mainly pyridinic, pyrrolic, and quaternary nitrogen, among others.[36, 55] Pyridinic groups contain sp^2-hybridized nitrogen atoms located at the edges or at defect sites of graphene sheets. In pyrrole, the sp^2-hybridized nitrogen is part of a five-membered ring structure. Quaternary nitrogen is assumed to substitute a carbon atom located in the graphene sheet with still unclear charge compensation, and pyridine-N-oxide originates from the oxidation of pyridinic nitrogen.

3.2 Interaction of surface defects with functional groups

The incorporation of heteroatoms inevitably introduces defects to CNTs. Oxygen is often anchored on the surface of CNTs by oxidative functionalization, although there are speculations that oxygen can be embedded in the bulk.[36, 47, 52] In contrast, it is much easier to incorporate nitrogen in the bulk graphitic structure of CNTs because nitrogen is capable of bonding with three carbon atoms as compared to two for oxygen.[35] An extreme case of nitrogen embedding in the bulk is carbon nitride, which, however, does not have the typical metallic conductivity and high surface area of carbon nanomaterials.[56]

Conversely, the presence of defects can enhance the amount and stability of anchored heteroatoms. Defects like carbon debris have a higher reactivity than graphitic carbon in gasification, i.e. combustion or methanation reactions,[57] through which heteroatoms can be incorporated. A recent study employed catalytic steam gasification or catalytic etching to create surface defects on CNTs.[58] Transmission electron microscopy and scanning tunneling microscopy investigations confirmed the introduction of surface defects, which also caused a clear change in the electronic structure of the CNTs as indicated by ultraviolet photoelectron spectroscopy measurements.[59] The etched CNTs were treated by nitric acid to obtain oxygen-containing functional groups. Temperature-resolved XPS detected a considerable increase in the amount and thermal stability of oxygen functional groups (Fig. 3), which undoubtedly demonstrated the effect of surface defects on binding oxygen species. Additional evidence was provided by temperature-programmed desorption studies with ammonia as a probe molecule, which revealed the adsorption of ammonia on defect sites.[59]

3.3 Interaction between O and N species at the gas-solid interface

OCNTs are often the starting materials for synthesizing NCNTs by post-treatment under ammonia. A series of surface reactions occur between ammonia and oxygen groups on the carbon surface, and the final surface chemistry depends mainly on the ammonia treatment temperature provided that sufficient reaction time is applied.[55] At treatment temperatures of up to 800 °C, a significant amount of oxygen remains in NCNTs.[36] Here, we should not overlook the role of defects in the incorporation of nitrogen species on oxygen-functionalized CNTs. As mentioned above, the oxygen functionalities and surface defects often form on carbon surface simultaneously. Studies on the gas-phase treatment with other nitrogen sources like aniline and ethylenediamine showed similar results, where oxygen species were always present on NCNT surfaces.[60]

In other studies, when polymers were used as nitrogen precursors for thermal treatment, oxygen was also detected on the obtained NCNTs.[61] In another example, polyaniline was coated on the OCNT surface in the liquid phase by cationic polymerization of aniline, and subsequent pyrolysis in the gas phase led to the formation of an amorphous carbon coating on CNTs (Fig. 4). Oxygen species were also unambiguously detected in the obtained NCNTs.[34] The presence of oxygen may also be related to the hygroscopic nature of CNTs. Oxygen may be incorporated through moisture during synthesis, storage or sample transfer for characterizations. The difference between post-treatment with ammonia and with N-containing hydrocarbon or polymers is that the treatment with the latter also results in carbon coating by pyrolysis, and nitrogen species are incorporated in the coated layer. In other words, the treatment using ammonia leads to the formation of nitrogen species mainly on the surface of carbon, while using N-containing hydrocarbon results in nitrogen species in surface layers, i.e., on the surface and in the bulk of the surface region. The latter is expected to be more durable in electrocatalytic applications under corrosive conditions.

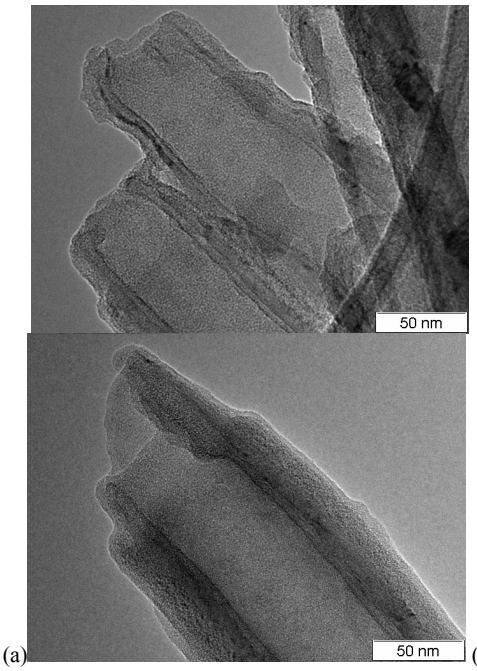

Fig. 4. NCNTs synthesized by treatment of OCNTs in aniline vapor at (a) 550 °C and (b) 850 °C. The rough surface indicates the presence of a nitrogen-containing carbon coating originating from the pyrolysis of aniline. Adapted from reference.[34]

3.4 Thermal stability of NCNTs and OCNTs as bulk materials

Thermal stability is a key issue for the application of carbon materials in catalysis. As a general rule, the oxidation resistance of carbon materials relies on their structure and purity. Any heteroatoms, impurities or defects introduced to the surface or the bulk of CNTs will lead to a decrease of their oxidation resistance. The corrosion of carbon materials is known to occur more rapidly at defect sites.[36] Several commonly used NCNT samples were studied by temperature-programmed oxidation (TPO) in the gas phase and compared with acid-washed CNTs and oxygen-functionalized CNTs. Catalytically grown NCNTs (NCNT-growth) showed a considerably lower oxidation resistance than all the other samples as indicated by the CO_2 peak at much lower temperatures (Fig. 5), which can be attributed to surface defects and structural disorders due to the presence of N in the carbon lattice.[62, 63] In contrast, CNTs purified by washing in diluted acid showed the highest thermal resistance among all the samples. Both oxygen functionalization (OCNTs) and the incorporation of nitrogen (NCNT-NH_3 and NCNT-aniline) led to a decrease of the oxidation resistance as indicated by CO_2 peaks at lower temperatures. The CO_2 peak position of NCNT-NH_3 is rather close to that of OCNTs, while the initial CO_2 release temperature of NCNT-NH_3 was higher than that of OCNTs, which is related to the decomposition of oxygen-containing groups on OCNTs. Hence, the bulk structure of OCNTs is similar to that of NCNT-NH_3 with differences only on the surface. Different from the surface effects introduced by the NH_3 treatment, the CO_2 peaks shifted to a higher temperature for NCNT-aniline, which can be related to the presence of a nitrogen-doped carbon coating or amorphous carbon on the surface.[34] The release of CO occurred at higher temperatures than that of CO_2 for all samples. The asymmetry of the peaks can be attributed to the decomposition of surface oxygen groups. It is remarkable that the NCNT-growth sample showed only a negligible CO peak. These results indicate that the thermal stability of CNTs is related to surface and bulk defects as well as to surface functional groups involving heteroatoms.

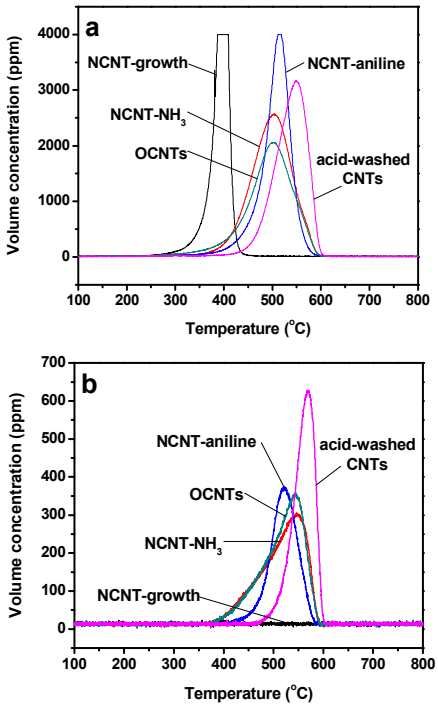

Fig. 5. (a) CO_2 and (b) CO profiles of acid-washed CNTs, OCNTs and NCNTs obtained by catalytic growth (CNT-growth), by post-treatment of OCNTs with ammonia (NCNT-NH_3) and with aniline vapour (NCNT-aniline). The measurements were carried out by heating 5.0 mg of sample from room temperature to 800 °C at a heating rate of 1 K min^{-1} in 5 vol % O_2 in helium. Adapted from reference.[60]

3.5 Thermal stability of oxygen and nitrogen groups on the surface

Apart from the oxidation resistance of different CNTs determined by TPO as a bulk material, the thermal stability of different functional groups on the surface varies as well. Carboxyl, hydroxyl and carbonyl groups are among the most common oxygen species on partially oxidized carbon materials. The ether-type oxygen or pyran can substitute one carbon atom at the edge, and aldehydes can also be present on the surface of the oxidized CNTs. Heating in inert or reducing atmosphere removes the surface functional groups step by step, and the type and amount of surface functional groups can be controlled by thermal treatments.[52] Surface-sensitive methods like XPS and temperature-programmed techniques are often employed to quantitatively determine the amount and type of surface oxygen and nitrogen groups. We performed TPD studies with ammonia as a probe molecule to investigate surface acidic groups (Fig. 6). The oxidized CNTs were pretreated at different temperatures in helium or in hydrogen. The TPD with pre-adsorbed ammonia quantitatively determined the acidic sites on the nitric acid-treated CNTs. The main ammonia desorption peak appeared at about 120°C (Fig. 6), indicating that most of the ammonia molecules are weakly chemisorbed. The shoulder at high temperatures can be assigned to carboxylic structures, onto which ammonia chemisorbs strongly presumably via the formation of ammonium carboxylates. Most of the acidic groups act as primary adsorption centres, which bind additional ammonia molecules weakly through hydrogen bonds.[53, 64] It can be seen clearly that the thermal treatment led to a decrease of acidic sites on CNTs, and the hydrogen atmosphere is more effective in removing surface oxygen groups (Fig. 6). While there were still considerable amounts of acidic groups left on CNTs after the pretreatment at 450 °C in helium, most of the acidic groups were removed in hydrogen at the same treatment temperature. In comparison, surface nitrogen groups are more stable than oxygen groups under inert atmosphere. It was reported that nitrogen species

are stable up to 670 °C under argon.[65] Similar results were reported in other studies.[66] Especially, graphite-like or quaternary nitrogen is more stable than any other nitrogen species in NCNTs.[65]

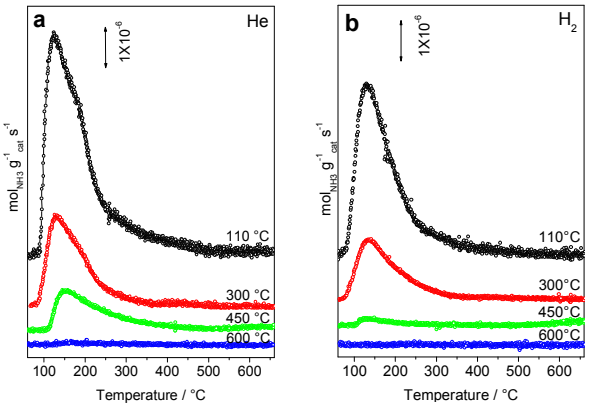

Fig. 6. Ammonia TPD profiles of nitric acid-treated CNTs measured under helium flow (100 sccm) using a heating ramp of 10 °C min^{-1}. The sample was pretreated at different temperatures in helium (a) and hydrogen (b) for 60 min prior to the adsorption of ammonia at 30 °C for 30 min. The reactor was purged with helium after adsorption.

3.6 Interaction between oxygen and nitrogen groups in the liquid phase

Nitrogen-doped CNTs with or without metals are known to be highly active in electrocatalytic oxygen reduction reaction (ORR) under alkaline conditions.[67] However, the electrochemical stability in the corrosive electrolyte is a major challenge for NCNTs, especially when a high potential is applied under reaction conditions. Furthermore, as a typical three-phase reaction the ORR proceeds only when sufficient contact among these phases can be achieved. For the efficient release of the produced H_2O in the ORR, the electrode has to be hydrophobic. Otherwise, the electrode can be flooded due to H_2O accumulation, and the diffusion of molecular oxygen will be impeded or even blocked leading to an increase of overpotential or to cell failure. Generally, the electrode for ORR needs to be hydrophobic to achieve effective water release. While nitrogen doping does increase the hydrophilicity of CNTs, OCNTs are even more hydrophilic in comparison. Nevertheless, nitrogen doping often involves pre-oxidation, for example, by HNO_3.[36] Even for directly grown NCNTs without pre-oxidation, oxygen and nitrogen groups as well as surface defects always coexist on NCNTs, which decrease the hydrophobicity and are unfavorable for the ORR. Hence, it is essential to understand the impact of the electrolyte on NCNTs used as electrocatalysts, especially on their surface properties under industrially relevant conditions.

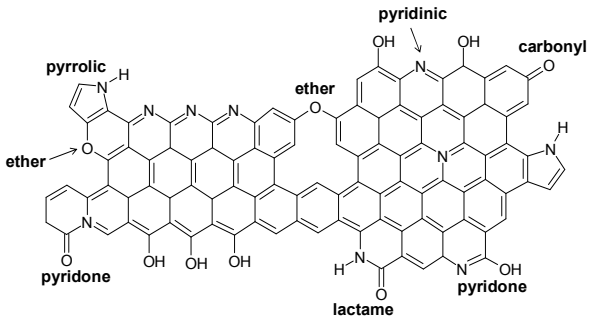

Fig. 7. Surface groups of three types of NCNTs after alkaline treatment. Adapted from reference.[60]

Three different types of NCNTs synthesized either by direct growth or by post-treatment using different precursors were treated in 10 M KOH at 80 °C for 5 h.[60] The NCNT samples before and after the alkaline treatment were characterized and tested with the focus on the initial activation and stabilization stage of the NCNTs. A significant increase in oxygen concentration was observed for all the samples after treatment in 10 M KOH. However, the nitrogen species appeared to be very stable under the applied alkaline conditions. Fig. 7 schematically shows the oxygen and nitrogen species that are presumably present on the treated NCNT surface. Detailed analysis shows that the incorporation of oxygen species on NCNTs by the applied alkaline treatment may follow three different pathways: (1) In case of large nitrogen-free areas, oxygen species attack carbon at defect sites preferably forming C−OH. (2) Nitrogen activates neighboring carbon atoms, which then anchor oxygen species forming C−OH or C=O. (3) When the surface is largely occupied by nitrogen and oxygen species like on NCNT-growth, nitrogen species may decompose upon attack by OH^- forming preferably C=O. Normal CNTs without nitrogen were also studied for comparison, and a strong increase of C−O was observed after the treatment. In contrast, the sample NCNT-growth showed a strong increase in C=O indicating that nitrogen species in NCNTs influence surface oxidation and the formation of oxygen groups on carbon. Generally, it is assumed that the species with oxygen and nitrogen on adjacent sites like pyridone and lactame are not high temperature-stable species. These species can be formed in the liquid phase upon alkaline treatment, but decompose at elevated temperatures in the gas phase. In other words, the stability of a certain group is higher when the surrounding crystalline graphitic structure is larger.

4. Interaction with water

The wetting properties of CNTs and NCNTs used in catalysis have strong impact on their performance. Wetting is often necessary for the deposition of nanoparticles on CNTs in aqueous solutions. In electrocatalytic oxygen reduction or evolution reactions, wetting properties may influence the release of water or gas bubbles. Actually, water management is a major challenge for fuel cell catalysis. During the oxygen reduction reaction, water forms on the catalyst surface in the electrode. The water molecules have to be removed from the electrode effectively. Otherwise, they will accumulate in the liquid phase, and at a certain stage the charge transfer may be hindered and the electrode may be flooded leading to unexpected breakdown of the cell. In case of the oxygen evolution reaction, water is oxidized to molecular oxygen, which has to be effectively released from the catalyst surface. The build-up of gas bubbles inevitably leads to an increase of electrode resistance and a decrease of catalytic efficiency. The release of water or molecular oxygen strongly relies on the surface properties of the electrode.

Water physisorption is a unique technique for the characterization of the surface wetting properties. The adsorption isotherms can be used to analyze the interaction between water molecules and sample surface and quantitatively determine the amount of adsorbed water. Hence, this technique was employed to characterize CNTs after different modifications. The measurement was performed at 25 °C. It can be seen from Fig. 8 that the CNTs with different modifications show clearly different adsorption-desorption behavior. A hysteresis is visible at high pressure for CNTs, and the adsorbed water amounts to 17.9 mmol g^{-1} in total indicating a relative hydrophobic surface. In contrast, the OCNTs adsorb water at much lower pressures and two hysteresis loops were observed. The one at lower pressure is related to the surface oxygen groups on OCNTs including carboxyl and hydroxyl groups, which can strongly interact with water molecules through hydrogen bond. The total amount of water adsorbed by OCNTs reached 28.3 mmol g^{-1}. As compared to CNTs, the sample NCNT-NH_3 adsorbed a slightly higher amount of water in total, i.e., 19.8 mmol g^{-1}. However, strong interaction with water was observed at lower pressure as indicated by the hysteresis at the relative pressure of around 0.5. Both oxygen and nitrogen groups on carbon surface can contribute to the adsorption of water molecules.

However, the interaction between oxygen-groups and water is stronger than that between nitrogen-groups and water due to stronger hydrogen bonds. The sample NCNT-growth showed a relatively high adsorption capacity of 26.6 mmol g^{-1}, while strong interaction at low relative pressure was not observed. All the three modified CNTs are more hydrophilic than the CNTs without surface modifications. In contrast to oxygen, nitrogen groups do not strongly interact with water. The sample NCNT-NH_3 prepared from OCNTs by post-treatment showed properties of both OCNTs and NCNT-growth, likely due to the presence of both oxygen and nitrogen groups in sufficiently high amount.

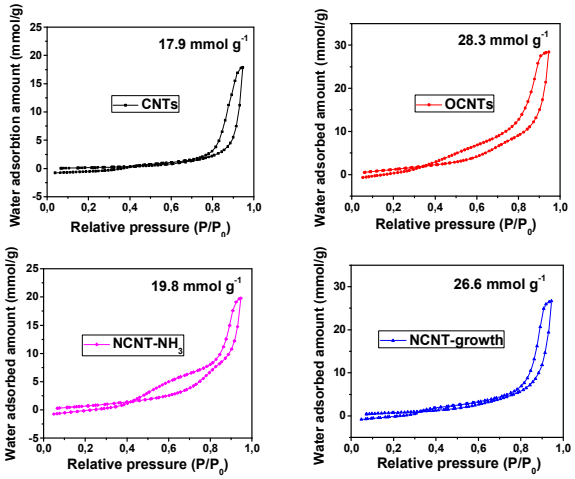

Fig. 8. Water physisorption isotherms of different CNTs. The measurements were performed at 25 °C. (a) purified CNTs obtained by washing with diluted HNO_3; (b) OCNTs obtained by HNO_3 vapor treatment of purified CNTs, treated at 200 °C for 24 h; (c) NCNTs obtained by NH_3 treatment of OCNTs, treated at 600 °C for 6 h; (d) catalytically grown NCNTs purified by diluted HNO_3.

5. Residual growth catalysts

The catalytic growth of CNTs usually involves metal catalysts with oxide or mixed oxides as support or matrix.[3, 68] The amount of impurities in produced nanotubes depends on their yield. The yield of NCNTs is much lower than that of conventional CNTs, and the amount of residual catalysts in NCNTs is therefore considerably higher than in CNTs.[69] The removal of these impurities often requires tedious purification procedures involving sequential washing by acid and/or base, and the difficulties in removing the impurities by acid treatment can be attributed to the sheathing of the metal nanoparticles by graphene layers.[70] As a result, the complete removal of the metal catalysts used for the CNT growth turns out to be very challenging or essentially not possible.[71] Hence, metal impurities are unavoidable due to the catalytic growth process used for the CNT synthesis.[72, 73]

In general, electrocatalysis is more sensitive to the metal impurities in CNTs and NCNTs. For example, even traces of metal species may have a significant impact on the electrocatalytic performance of N-doped carbon materials in the oxygen reduction reaction. In contrast, catalytic reactions in the gas phase are less sensitive. Exposed metal species can be largely removed by repeated washing, and the catalytic effect of the purified CNTs or NCNTs is often not detectable any more, although encapsulated metals can still be detected by elemental analysis.

5.1 Role of residual metal species in gas phase reactions

Residual metal species may be used as active phase for catalytic reactions. For example, it was reported that residual Co and Fe catalysts showed superior activities in NH_3 decomposition.[74] While only a limited number of reactions were reported using the residual metal species as active phase in gas phase catalytic reactions, the role of residual metals is far more profound. As discussed above, oxygen- and nitrogen-containing functional groups are essential for the application of CNTs. Recent studies show that metal species in CNTs influence the decomposition of surface functional groups. For example, during the thermal decomposition of surface oxygen groups, the reverse Boudouard reaction (Eqn. 1) occurs forming CO by the gasification of carbon materials with CO_2.[75] Group VIII metals, alkali and alkaline-earth salts are known to be highly active catalysts for the Boudouard reaction.[76] The reaction involves a redox cycle of the applied VIII metal with CO_2 as oxidizing agent and C as reducing agent.

$$CO_2 + C \rightleftharpoons 2\ CO \qquad (1)$$

The TPD profiles of the samples OCNT-L (oxidized in liquid HNO_3, washed and largely free of exposed metal residues) and OCNT-V (oxidized in HNO_3 vapor, without washing, with exposed metal residue) in helium are shown in Fig. 9.[72] The desorption of CO_2 below 340 °C can be attributed to the decomposition of carboxylic acid groups, and the peaks at around 480 °C and 640 °C are due to the decomposition of more stable groups like carboxylic anhydrides and lactones, respectively. In the CO profile, desorption below 300 °C can be assigned to aldehydes. The decomposition of carboxylic anhydride groups also gives rise to CO production at the same temperature of 480 °C as observed for CO_2. The desorption of CO at 700 °C is related to the decomposition of phenol and ether groups. Carbonyls decompose at an even higher temperature of around 830 °C. CO_2 desorption was not observed above 750 °C in both samples. A sharp CO desorption peak at 730 °C was obtained with sample OCNT-V (oxidized in HNO_3 vapor, without washing, with exposed metal residue), which did not appear for OCNT-L (oxidized in liquid HNO_3, washed and largely free of exposed metal residues). Moreover, the increase in the CO concentration is accompanied by a decrease in the CO_2 concentration. Hence, the CO peak observed for sample OCNT-V at ca. 730 °C can be assigned to a pronounced gasification reaction with residual metal species as catalysts. This is to say, CO_2 released from the thermal decomposition of surface groups was reduced to CO by carbon, and the reaction occurred only when metal residues were present.

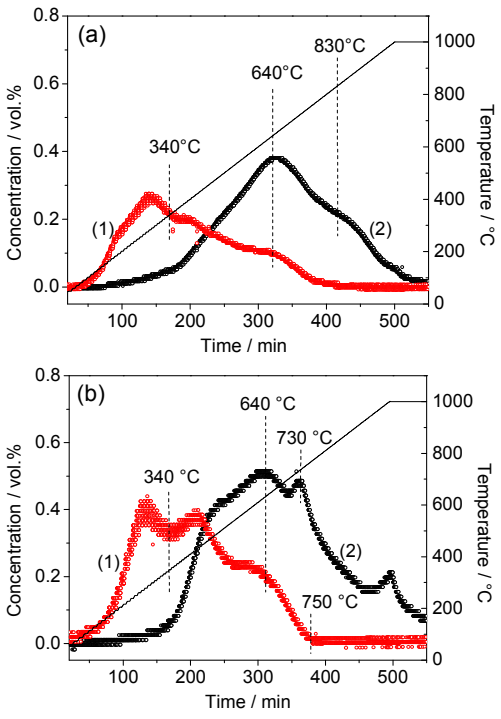

Fig. 9. TPD profiles of (a) OCNT-L (oxidized in liquid HNO_3, washed and largely free of exposed metal residues) and (b) OCNT-V

(oxidized in HNO_3 vapor, without washing, with exposed metal residue) performed in helium at a heating rate of 2 K min^{-1}. (1) CO_2; (2) CO. Adapted from reference.[72]

5.2 Role of residual metal species in electrocatalysis

As compared to gas-phase reactions, electrocatalysis is more sensitive to metal impurities, and even traces of metal species may have a significant influence on the catalytic performance. Consequently, a large number of publications on CNTs reporting metal-free catalysts for the oxygen reduction reaction may have been influenced by traces of metals. The role of residual metal species present in "metal-free" carbon catalysts has been under continuous debate in the last years.[77]

Compton and co-workers [78, 79] found that the residual growth catalyst in CNTs caused the electrocatalysis phenomenon associated with the CNT-modified electrodes, and pointed out that the electrocatalytic activity of CNTs in the reduction of hydrogen peroxide was due to the residual iron oxide impurities. Stevenson and coworkers [40] pointed out that in nitrogen-containing carbon catalyst prepared by pyrolysis, nitrogen species are only responsible for two electron transfer by reducing molecular oxygen to hydrogen peroxide, and further reduction or disproportionation relies on metal species. Density functional theory studies confirmed this mechanism and demonstrated the importance of metal species even in traces.[80]

While the encapsulated residual growth catalysts may not be removed by acid washing, they can be exposed by oxidative thermal scission. As shown in a recent study, the thermal oxidative treatment of catalytically grown NCNTs containing encapsulated Co and Mn oxide nanoparticles simultaneously ruptures the NCNTs and oxidizes the Co and Mn oxide nanoparticles forming spinel Co-Mn oxides nanoparticles partially embedded in the NCNTs.[81] Fig. 10 shows the development of the phases of the mixed oxides in NCNTs as a function of thermal cutting temperature. The buildup of the spinel phase was clearly observed after thermal cutting and the intensity increases with increasing cutting temperature. Due to a synergetic effect of the nitrogen groups and the spinel Co-Mn oxide, the resulting catalysts showed exceptional activity and stability when used as bi-functional electrocatalysts in reversible oxygen electrodes under alkaline conditions.

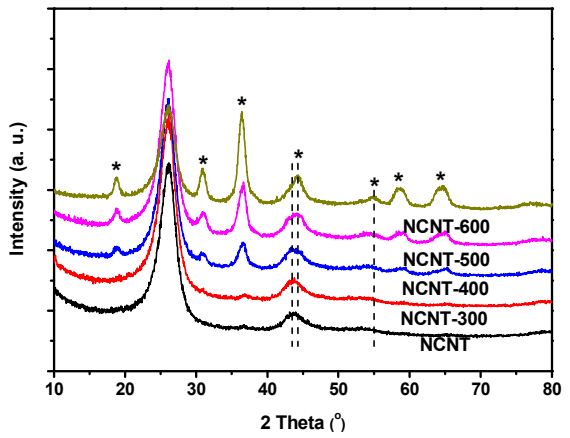

Fig. 10. XRD patterns of NCNT samples after oxidative cutting under flowing air at different temperatures. The oxidation was performed by moving the reactor to a preheated furnace and kept for 5 min before moving it out of the heating zone. The NCNTs were synthesized using Co-Mn-based mixed oxide catalysts. The spinel phase of Co-Mn oxide is identified by * in the diffraction patterns. Adapted from reference.[81]

To verify the effect of trace metal species in electrocatalysis, Masa et al. [71, 73] performed a careful synthesis of a metal-free nitrogen-doped carbon catalyst, cautiously avoiding any metal contamination. Metal precursors in minute concentrations (0.05–1.05 wt.%) were then deliberately incorporated and the resulting effect on the ORR was investigated. Electrocatalytic investigations disclosed that the metal-free catalyst did not show as high ORR activity as the catalysts that were prepared by deliberate addition of trace metal precursors. In particular, the addition of Fe to the metal-free catalyst in concentrations of as low as 0.05% significantly influenced the activity and selectivity of the electrocatalyst. These findings demonstrate the important role of metal species even in trace amounts that are not detectable by many common surface-sensitive techniques including XPS.[71]

6. Dispersion and sintering of supported metal nanoparticles

6.1 Influencing factors and correlations

The deposition of metal nanoparticles on carbon can be achieved by electrostatic or chemical interactions between metal precursor and carbon surface. In both cases, surface functionalities or defects play an essential role.[82, 83] As mentioned above, both the oxygen- and nitrogen-containing groups can act as anchoring sites for foreign species, and both can improve the wetting properties of CNTs, which is essential for the deposition of metal particles from the liquid phase, for example, by impregnation.[84-87] However, it is the difference between oxygen and nitrogen species that determines the dispersion and sintering of supported metal or oxide nanoparticles. Oxygen groups interact more strongly with H_2O molecules as indicated by water adsorption studies (see Fig. 8). Oxygen species are mainly functional groups attached to the carbon surface, while nitrogen species can be more easily incorporated in the graphitic structure of carbon. As a result, nitrogen tends to create surface or bulk defects in the graphitic structure, while oxygen is more grafted on the surface as functional groups. More importantly, as anchoring sites for metal particles, their thermal stability is very different: Nitrogen species are far more stable than oxygen species. Obviously, these features are correlated. The form of chemical bonding determines the defect level, and consequently the thermal stability and interaction with foreign molecules. Due to these differences between oxygen and nitrogen species on CNTs, different metal dispersion was often observed on OCNTs and NCNTs when preparing under identical conditions, and the sintering of metal particles upon heating occurs to different extents on OCNTs and NCNTs.

We have studied the deposition of metal or oxide particles on OCNTs and NCNTs in the last few years. Different synthesis routes were employed including impregnation, precipitation and chemical vapour deposition. Both noble metals such as Pt, Pd, and Ru and non-noble metals such as Fe and Co were investigated. All these studies demonstrated that the dispersion of metal or oxide nanoparticles is higher on NCNTs than on OCNTs. Furthermore, the thermal stability against sintering upon heating is also higher on NCNTs. Despite of similar trends, the structural and electronic properties of metal nanoparticles can be influenced differently by OCNTs and NCNTs as support materials.

6.2 Pd nanoparticles on modified CNTs

In situ TEM and spectroscopic methods were employed by Su and coworkers [88] to investigate the interaction between palladium and modified CNTs in a model system. It was found that the stability of palladium nanoparticles supported on CNTs depends strongly on the surface properties of CNTs. The surface functional groups could decrease the point of zero charge of CNTs and promote the adsorption of cationic Pd complex.[89] When used as catalyst for direct H_2O_2 synthesis, Pd appeared to be mobile on NCNTs.[90] The deposition of Pd nanoparticles in the inner surface of CNTs improved their thermal stability against sintering.[91] In addition to Pd oxide, divalent polynuclear Pd_n-hydroxo complexes may form on the carbon surface.[92] As another example, Pd nanoparticles were

deposited on OCNTs and NCNTs from colloids, which were synthesized using Pd(II) acetate as precursor and methanol as stabilizer and reductant.[93] Elemental anaylsis showed that the Pd loadings on OCNTs and NCNTs were 0.89 wt% and 0.63 wt%, respectively.[94] The different Pd loadings on OCNTs and NCNTs can be related to the differences in the total amount of anchoring sites generated by the oxygen and nitrogen functionalization. The XRD patterns of Pd/OCNT and Pd/NCNT samples reduced at 200 °C in H_2 are displayed in Fig. 11. The hexagonal graphite structure of the CNTs was detected in both samples with reflections at around 26° and 42°. For the sample Pd/OCNT, three weak peaks at 40°, 47° and 68° were detected, which are identified as the Pd(111), Pd(200) and Pd(220) reflections, respectively. In contrast, only a weak and broad contribution at around 40° corresponding to Pd(111) was observed for Pd/NCNT. The stronger reflections on OCNTs indicate larger Pd particles on OCNTs than on NCNTs. The result was confirmed by further studies using H_2 chemisorption. The H/Pd ratio (H adsorbed on surface Pd sites) was 0.37 on NCNTs in contrast to 0.23 on OCNTs.[94] Despite the lower Pd loading on NCNTs, the dispersion was found to be higher on NCNTs than on OCNTs.

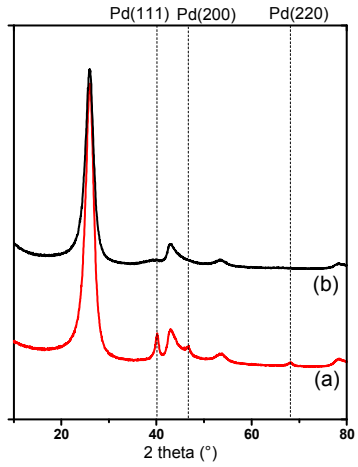

Fig. 11. XRD patterns of (a) Pd/OCNT and (b) Pd/NCNT. The samples were prepared by a colloidal method followed by reduction in H_2 at 200 °C. Adapted from reference.[94]

6.3 Pt nanoparticles on modified CNTs

Similar results were also observed for Pt nanoparticles, which were deposited on modified CNTs by a non-aqueous impregnation method.[95] $H_2PtCl_6 \cdot xH_2O$ was used as precursor with ethanol as solvent. Elemental analysis disclosed that the loading of Pt is slightly higher on OCNTs (3.0 wt%) than on NCNTs (2.8 wt%).[96] To investigate the metal-support interactions, two different reduction temperatures of 200 °C and 400 °C were applied. XRD results indicate that for both reduction temperatures, the Pt particle size is larger on OCNTs than on NCNTs. The reduction at 400 °C led to a clear increase of Pt reflections in the sample Pt/OCNT, while the XRD pattern remains unaffected for Pt/NCNT. Hence, surface nitrogen groups inhibit the sintering of Pt nanoparticles upon heating indicating stronger metal-support interactions on NCNTs than on OCNTs. These results were confirmed by TEM studies, and the particle size distribution was found to be narrower on NCNTs than on OCNTs.[96]

Several factors have contributed to the less severe sintering on NCNTs than on OCNTs including the higher thermal stability of nitrogen groups, the strong metal-nitrogen interaction and the surface defects created due to incorporation of nitrogen in carbon. It is known that nitrogen-containing surface groups are significantly more stable than oxygen-containing groups.[36, 66] Therefore, thermal treatment does not cause a significant loss of anchoring sites on NCNTs, which is not the case on OCNTs. The presence of these anchoring sites can help securing the nanoparticles on their original positions thus prohibiting them from sintering upon heating. The strong metal-nitrogen bond enhanced metal-support interactions limiting the coalescence of neighbouring nanoparticles. As to the defects, edge planes typically present on the nitrogen-doped carbon surface may help hindering the mobility of the nanoparticles.

6.4 Influence of the applied atmosphere on the sintering of iron nanoparticles on NCNTs

We have shown that the atmosphere used in the thermal treatment has significant influence on the sintering behaviour of iron nanoparticles on NCNTs.[97] Iron oxide nanoparticles supported on NCNTs were synthesized by chemical vapour deposition (CVD) from ferrocene under oxidizing conditions. A theoretical Fe loading of 6 wt% was applied, and elemental analysis indicates that the obtained Fe loading was 3.96 wt%. TEM studies disclosed that very small nanoparticles with diameters of 1-2 nm were obtained (
Fig. 12a). The sintering experiments were performed at 500 °C for 1 h in helium, hydrogen or ammonia flow. After thermal treatment in helium, a significant increase in particle size was observed with particles as large as 15 nm (
Fig. 12b). Particularly, the particle size distribution was significantly widened. Different from helium, the thermal treatment in hydrogen led to very homogeneous nanoparticles with narrow size distribution as shown in
Fig. 12c. Obviously, the sintering in hydrogen is less severe than in helium. Thermal treatment in ammonia led to the minimum sintering of the nanoparticles (
Fig. 12d), where the obtained particles are clearly smaller than in the samples treated in hydrogen. As compared to OCNTs, the nanoparticles are smaller on NCNTs both before and after sintering under different atmospheres at 500 °C.

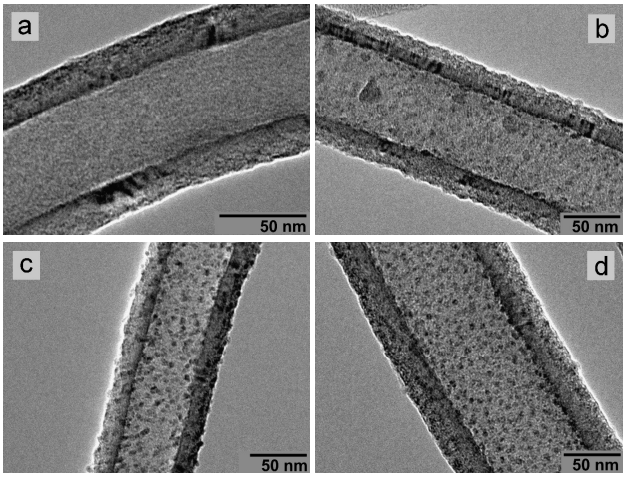

Fig. 12. TEM images of iron nanoparticles deposited on NCNTs by CVD method with a Fe loading of 3.96 wt%. The as-synthesized samples (a) were treated at 500 °C for 1 h under different atmospheres including helium (b), hydrogen (c), and ammonia (d). Adapted from reference.[97]

XRD studies confirmed the growth of particles during the thermal treatment and disclosed the presence of ε-Fe_3N-type nitride in the sample treated with ammonia.[97] The differences in sintering in different treatment atmospheres were further confirmed by XPS investigations. It can be seen from Table 1 that the as-synthesized samples have the highest Fe concentration, and the Fe concentration is always higher on NCNTs than on OCNTs. All the thermal treatments caused sintering of the iron nanoparticles and the

decrease of the surface atomic concentration of Fe. The most significant decrease was observed for the treatment in helium, while the treatment in ammonia caused the least decrease.

Table 1. Surface atomic concentrations derived from XPS studies. Iron nanoparticles were deposited on NCNTs by CVD method with a Fe loading of 3.96 wt%. The thermal treatment was performed at 500 °C for 60 min in different atmospheres. Adapted from reference.[97]

treatment	as is	He	H_2	NH_3
Fe at.%	7.1	4.6	5.0	6.1

These results show the applied atmosphere has a significant influence on the sintering behaviour of the Fe nanoparticles on modified CNTs. Treatment in helium led to significant sintering and widening of particle size distributions, which can be related to the reaction between iron oxide and carbon, i.e., the high temperature carbothermal reduction: Iron oxide can be reduced by the carbon substrate in inert atmosphere forming metallic Fe at high temperatures (Eq. 2). Additionally, the reaction at the particle-substrate interface can enhance the mobility of the nanoparticles leading to sintering. However, in hydrogen and ammonia the nanoparticles were reduced by the applied reduction gas at lower temperatures compared with the carbothermal reduction. Furthermore, metallic iron can hardly react with the carbon substrate under reducing conditions at the applied temperatures, and the particles are therefore less mobile. As a result, the sintering of the nanoparticles was less severe in hydrogen and ammonia, and substantial widening of particle size distributions was not observed.

$$Fe_2O_3 + 3C \rightarrow 2Fe + 3CO \quad (2)$$

7. Chemical state of metal nanoparticles on modified CNTs

7.1 Substrate effect on metal reduction

The strong metal-support interaction may be reflected by the modification of the chemical state of supported metal nanoparticles. The effect is especially noticeable for small particles of a few nanometers in close contact with the substrate. In the last few years, we have compared the differences in the oxidation state of supported Pd, Pt, Fe, Co and Mn nanoparticles on OCNTs and NCNTs. Mainly XPS was employed for the investigations.

A typical example is Pd on modified CNTs with less than 1 wt% Pd loading.[98] The OCNTs used as support contain 4.8 at% oxygen on the surface, while NCNTs contain 1.6 at% nitrogen and 2.7 at% oxygen, as disclosed by XPS studies. The Pd/CNT samples were investigated in the as-prepared (colloidal method, after drying) as well as reduced state (H_2, 200 °C). Three major contributions can be distinguished in the Pd $3d_{5/2}$ spectra. The contributions at ca. 335.5 eV can be assigned to metallic Pd.[99] Pd at slightly higher oxidation state was detected at 336.5 eV. The contribution at ca. 338 eV originates from $Pd(OAc)_2$, that is, the precursor used for the synthesis. It can be seen that the oxidation state of Pd on OCNTs and NCNTs differs significantly in the as-prepared samples (Fig. 13). Pd on NCNTs is largely in the reduced state, whereas it is in a more oxidized state on OCNTs in the as-prepared samples.[94] The higher reduction degree on NCNTs reflects the substrate effect, that is, NCNTs favour the formation of metallic Pd. Reduction at 200 °C caused a significant increase of Pd^0 in Pd/OCNT, and the overall Pd intensity was boosted after reduction especially in Pd/NCNT likely due to the removal of surface organic species including functional groups. Quantitative analysis disclosed that the Pd dispersion was higher on NCNTs than on OCNTs, which is in good agreement with the XRD and TEM results.[94]

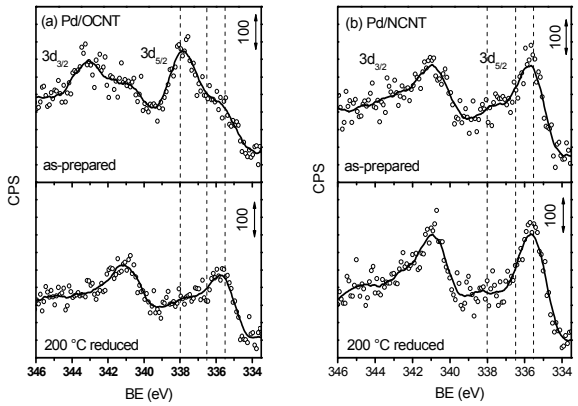

Fig. 13. XP Pd 3d spectra of (a) Pd on OCNTs and (b) Pd on NCNTs. As-prepared samples and samples after reduction in H_2 at 200 °C are shown. Adapted from reference.[94]

7.2 Re-oxidation of support and catalyst

While Pd deposited on OCNTs can be reduced to the metallic state by hydrogen, an oxidation treatment can re-introduce oxygen to the surface of Pd/CNT catalysts. By again generating oxygen species, the surface polarity and acidity of the Pd/CNT catalysts can be modified to achieve favourable results in catalysis.[100] However, due to the presence of deposited Pd nanoparticles, the oxidation treatment cannot be performed by refluxing in nitric acid as conventionally performed for CNTs. Under these conditions, the oxidation with nitric acid vapour turned out to be an interesting alternative, and the treatment was performed under much milder conditions as compared to typical treatment for CNT functionalization to avoid leaching and significant sintering of Pd nanoparticles.[101] Fig. 14 shows the normalized XPS spectra with deconvoluted O 1s region. The Pd $3p_{3/2}$ signal in the O 1s region was fitted using the Pd $3p_{1/2}$: $3p_{3/2}$ peak ratio of 1:2.[102] The normalized spectra clearly demonstrate an increase in the amount of oxygen-containing groups on the carbon nanofiber (CNF) surface after the gas-phase oxidation (GPO) treatment as revealed by an increase in the O 1s peak as a function of the treatment time. After 15 h similar increases in both the C-O and C=O signals were detected. For longer treatment durations the increase of the C-O signal is more significant as compared to that of the C=O signal indicating that with longer treatment time more phenolic and ether type groups were introduced. Not surprisingly, the nitric acid vapour treatment of the Pd/CNF catalysts also caused the oxidation of Pd. As can be seen from Fig. 15, Pd was found to be dominantly at higher oxidation state in the oxidized sample. The formation of palladium oxide species during oxidation is not regarded as a major problem for the following catalytic applications where metallic Pd is needed. Noble metals like palladium are known to be easily reducible at relatively low temperatures or even at room temperature.[103] As disclosed by XPS studies, the Pd nanoparticles regained the metallic state after reduction in hydrogen at low temperature (Fig. 15). In contrast, the introduced oxygen species were not significantly affected because the oxygen groups start to decompose at temperatures higher than 200 °C typically.[36, 52] Hence, the nitric acid vapour treatment of Pd/CNF increased the polarity and surface acidity but simultaneously maintained the active surface of Pd. As a whole, the oxidation treatment significantly enhanced the catalytic performance of Pd/CNF in the deoxygenation of amphiphilic fatty acid.[100]

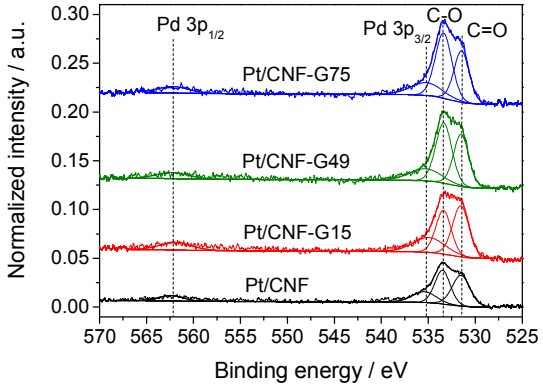

Fig. 14. XP Pd 3p and O 1s spectra of Pd nanoparticles supported on carbon nanofibers (Pd/CNF) oxidized by nitric acid vapour treatment. Concentrated HNO_3 was heated to 100 °C and the sample was kept at 125 °C for the treatment. The treatment time was varied from 15 to 75 h and denoted as Pd/CNF-Gx with x indicating the applied time in hours. The samples were dried at 125°C in air for 2 h before the XPS measurements. Pd/CNF-ox indicates the sample before treatment. Adapted from reference.[101]

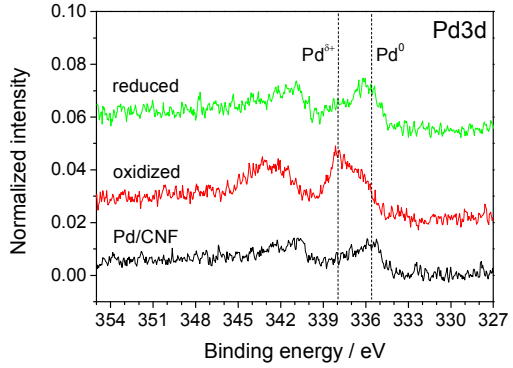

Fig. 15. XP Pd 3d spectra of Pd nanoparticles supported on carbon nanofibers (Pd/CNF) oxidized by nitric acid vapour treatment and subsequently reduced in hydrogen.

7.3 Metal-nitrogen bonding

It has been shown above that NCNTs promote the reduction of supported metal species and impede their sintering upon heating, which is assumed to be related to strong metal-nitrogen bonds. The formation of metal-nitrogen bonds like Fe-N has been observed using extended X-ray absorption fine structure (EXAFS) studies.[104] While the direct bonding between Pd or Pt with N was seldom detected, for example, by XPS, we did observe the metal-nitrogen bonding for non-noble transition metals including Fe, Co and Mn. As an example, FeO_x/NCNT was synthesized by chemical vapour deposition under oxidizing conditions, and thermal treatment was subsequently performed under helium and ammonia at 500 °C. All the samples show characteristic Fe $2p_{3/2}$ peaks at 711 eV indicating the presence of Fe^{3+} species. The as-prepared sample shows dominantly Fe^{3+} due to the applied oxidizing conditions using air. Additional contributions appear at 707.3 eV in the samples treated in ammonia (Fig. 16, NH_3), which can be assigned to Fe nitride species.[97] Fe-N species were also detected in the FeO_x/NCNT sample after treatment in helium, as revealed by the clear peak at 707.3 (Fig. 16, He). Since the treatment was performed in helium in this sample, the surface nitrogen groups other than ammonia are the nitrogen source for the metal-nitrogen bond formation. As compared to Fe-O, Fe in Fe-N has a higher electron density due to the lower electronegativity of N in comparison to O.

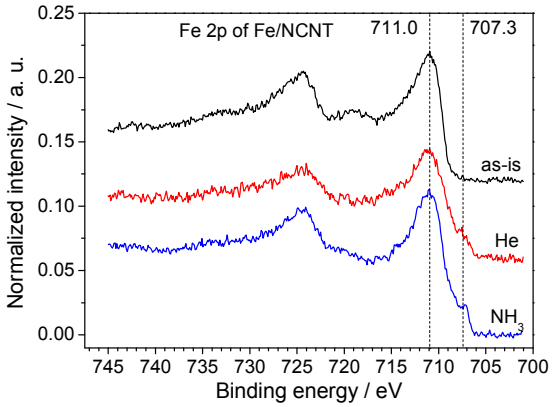

Fig. 16. XP Fe 2p spectra of FeO_x/NCNT samples after treatment at 500 °C for 60 min under different atmospheres. Adapted from reference.[97]

The direct metal-nitrogen interaction was also observed for Co deposited on nitrogen-doped carbon black. First, polypyrrole was deposited on carbon black from pyrrole and the sample was treated in inert gas at 800 °C to obtain the N-doped carbon black. Co was then incorporated by impregnation of a substituted cobalt porphyrin followed by thermal treatment at 650 °C under helium flow.[71] As can be seen from the XP Co 2p spectrum in Fig. 17, a clear shoulder appeared at 778.8 eV. While the main peak at about 789.7 eV indicates that Co mainly exists in oxide form, the low binding energy shoulder implies the presence of Co-N bonds. This result is in good agreement with literature studies where it has been suggested that the Co-N4 core of cobalt-N4 macrocyclic complexes is preserved after pyrolysis of the complexes at moderate temperatures.[105] Other studies in electrocatalysis also suggested that the Co-N4 moiety was formed during pyrolysis of a mixture of a nitrogen-rich organic compound or polymer and a suitable cobalt precursor supported on carbon.[106, 107] All these results are unambiguous evidence for the presence of strong metal-support interactions on nitrogen-doped carbon materials.

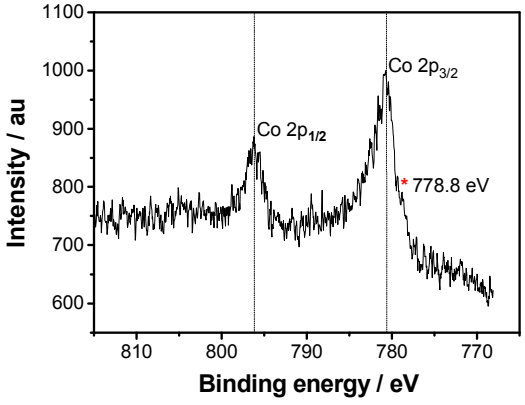

Fig. 17. High resolution XP Co 2p core-level spectra of Co supported on nitrogen-doped carbon black. The N-doped carbon black was synthesized by thermal treatment of polypyrrole-coated carbon black at 800 °C. Co was deposited by impregnation of a substituted cobalt porphyrin followed by thermal treatment at 650 °C under helium flow. The shoulder at the low binding energy side is assumed to be related to Co-N species. Adapted from reference.[71]

8. Summary

Carbon nanotubes have proved to be among the most versatile nanomaterials in the last two decades. Nitrogen functionalization or doping considerably broadened the scope of their application in catalysis due to manifold surface properties, among others. The concurrent presence of nitrogen and oxygen groups, surface defects and metal impurities although complicates the understanding and interpretation of the functioning of these systems on the one hand, they provide additional possibilities for tuning the dispersion, morphology, crystal structure, electronic structure, charge mobility, stability, and ultimately , the catalytic performance of supported metal nanoparticles on the other hand. Based on our own research and selected literature results, this review summarizes evidence for the following key statements:

1) NCNTs contain both nitrogen and oxygen groups especially when using a reductive treatment in ammonia of OCNTs to obtain NCNTs. Nitrogen exists both within the graphene sheets and on the surface, while oxygen species are mostly functional groups bound to the carbon surface.
2) The incorporation of any heteroatom in CNTs causes a decrease of thermal stability in air. Catalytically grown NCNTs are thermally less stable in air than OCNTs due to a more defective bulk structure and a higher amount of residual metal species.
3) Nitrogen species have a significantly higher thermal stability than oxygen groups in inert gas atmosphere.
4) Surface defects enhance the thermal stability of oxygen functional groups.
5) While both oxygen and nitrogen species lower the conductivity of graphitic carbon, NCNTs are more conductive than OCNTs.
6) Both oxygen and nitrogen groups interact with water and improve the wetting properties of CNTs. Oxygen groups interact more strongly with water than nitrogen groups.
7) Residual metal species promote the decomposition of surface functional groups and catalyse the total oxidation of CNTs.
8) Electrocatalytic oxygen reduction reaction is more sensitive to residual metal species than gas-phase reactions.
9) Both oxygen- and nitrogen-containing groups can act as anchoring sites for metal nanoparticles. Owing to a higher number of total anchoring sites, the metal loading can be slightly higher on OCNTs than on NCNTs for the same preparation conditions.
10) The degree of dispersion and the thermal stability of metal nanoparticles are higher on NCNTs than on OCNTs mainly due to the higher thermal stability of nitrogen species as anchoring sites.
11) NCNTs favour the formation of metal species in a lower oxidation state due to metal-nitrogen bonding, while on OCNTs the oxidation state of metal species is often higher.

Acknowledgements

Financial support from the German Ministry of Education and Research (BMBF) for the projects CarboScale (Grant 03X0040G), CarboElch (Grant 03X0207C), CarboKat (Grant 03X0204D) and SusHy (Grant 03X3581D) is gratefully acknowledged.

Notes and references

Laboratory of Industrial Chemistry, Ruhr-University Bochum, D-44780 Bochum, Germany.

Email: wei.xia@techem.rub.de, Fax: +49 234 32 14115

1. Q. Zhang, J.-Q. Huang, M.-Q. Zhao, W.-Z. Qian and F. Wei, *ChemSusChem*, 2011, **4**, 864-889.
2. J.-P. Tessonnier and D. S. Su, *ChemSusChem*, 2011, **4**, 824-847.
3. J. H. Bitter, *J. Mater. Chem.*, 2010, **20**, 7312-7321.
4. G. Centi and S. Perathoner, *ChemSusChem*, 2011, **4**, 913-925.
5. J. Zhu, A. Holmen and D. Chen, *ChemCatChem*, 2013, **5**, 378-401.
6. L. Yang, Y. Zhao, S. Chen, Q. Wu, X. Wang and Z. Hu, *Chinese J. Catal.*, 2013, **34**, 1986-1991.
7. I. Thome, A. Nijs and C. Bolm, *Chem. Soc. Rev.*, 2012, **41**, 979-987.
8. S. W. Kim, T. Kim, Y. S. Kim, H. S. Choi, H. J. Lim, S. J. Yang and C. R. Park, *Carbon*, 2012, **50**, 3-33.
9. P. Ayala, R. Arenal, M. Ruemmeli, A. Rubio and T. Pichler, *Carbon*, 2010, **48**, 575-586.
10. H. Wang, T. Maiyalagan and X. Wang, *Acs Catalysis*, 2012, **2**, 781-794.
11. S. R. Stoyanov, A. V. Titov and P. Kral, *Coordination Chem. Rev.*, 2009, **253**, 2852-2871.
12. Y. Shao, J. Sui, G. Yin and Y. Gao, *Appl. Catal. B*, 2008, **79**, 89-99.
13. B. Wang, *J. Power Sources*, 2005, **152**, 1-15.
14. D. W. Wang and D. S. Su, *Energy & Environ. Sci.*, 2014, **7**, 576-591.
15. S. Guo, S. Zhang and S. Sun, *Angew. Chem.-Int. Ed.*, 2013, **52**, 8526-8544.
16. K. Chizari, A. Deneuve, O. Ersen, I. Florea, Y. Liu, D. Edouard, I. Janowska, D. Begin and C. Pham-Huu, *ChemSusChem*, 2012, **5**, 102–108.
17. S. van Dommele, K. P. de Jong and J. H. Bitter, *Top Catal*, 2009, **52**, 1575–1583.
18. K. Zhou, B. Li, Q. Zhang, J.-Q. Huang, G.-L. Tian, J.-C. Jia, M.-Q. Zhao, G.-H. Luo, D. S. Su and F. Wei, *ChemSusChem*, 2014, **7**, 723–728.
19. P. R. Chen, L. M. Chew, A. Kostka, K. P. Xie, M. Muhler and W. Xia, *J Energy Chem.*, 2013, **22**, 312–320.
20. J. Zhang, X. Liu, R. Blume, A. Zhang, R. Schlögl and D. S. Su, *Science*, 2008, **322**, 73-77.
21. L. M. Ombaka, P. Ndungu and V. O. Nyamori, *Catal. Today*, 2013, **217**, 65-75.
22. P. Serp, M. Corrias and P. Kalck, *Appl. Catal. A*, 2003, **253**, 337–358.
23. J. M. Planeix, N. Coustel, B. Coq, V. Bretons, P. S. Kumbhar, R. Dutartre, P. Geneste, P. Bernier and P. M. Ajayan, *J. Am. Chem. Soc.*, 1994, **116**, 7935–7936.
24. K. Chizari, I. Janowska, M. Houllé, I. Florea, O. Ersen, T. Romero, P. Bernhardt, M. J. Ledoux and C. Pham-Huu, *Appl. Catal. A*, 2010, **380**, 72-80.
25. S. Maldonado, S. Morin and K. J. Stevenson, *Carbon*, 2006, **44**, 1429–1437.
26. S. W. Pattinson, V. Ranganathan, H. K. Murakami, K. K. K. Koziol and A. H. Windle, *Acs Nano*, 2012, **6**, 7723–7730.
27. S. van Dommele, A. Romero-Izquirdo, R. Brydson, K. P. de Jong and J. H. Bitter, *Carbon*, 2008, **46**, 138–148.
28. B. G. Sumpter, V. Meunier, J. M. Romo-Herrera, E. Cruz-Silva, D. A. Cullen, H. Terrones, D. J. Smith and M. Terrones, *Acs Nano*, 2007, **1**, 369–375.
29. A. A. Koós, M. Dowling, K. Jurkschat, A. Crossley and N. Grobert, *Carbon*, 2009, **47**, 30–37.
30. T. Sharifi, F. Nitze, H. R. Barzegar, C. W. Tai, M. Mazurkiewicz, A. Malolepszy, L. Stobinski and T. Wagberg, *Carbon*, 2012, **50**, 3535–3541.
31. K. Chizari, A. Vena, L. Laurentius and U. Sundararaj, *Carbon*, 2014, **68**, 369–379.
32. R. Arrigo, M. Hävecker, R. Schlögl and D. S. Su, *Chem. Commun.*, 2008, 4891-4893.
33. R. Chetty, S. Kundu, W. Xia, M. Bron, W. Schuhmann, V. Chirila, W. Brandl, T. Reinecke and M. Muhler, *Electrochimica Acta*, 2009, **54**, 4208–4215.
34. C. Jin, T. C. Nagaiah, W. Xia, B. Spliethoff, S. Wang, M. Bron, W. Schuhmann and M. Muhler, *Nanoscale*, 2010, **2**, 981-987.
35. I. Florea, O. Ersen, R. Arenal, D. Ihiawakrim, C. Messaoudi, K. Chizari, I. Janowska and C. Pham-Huu, *J. Am. Chem. Soc.*, 2012, **134**, 9672-9680.
36. C. Li, A. Zhao, W. Xia, C. Liang and M. Muhler, *J. Phys. Chem. C*, 2012, **116**, 20930-20936.
37. S. V. Dommele, A. Romero-Izquirdo, R. Brydson, K. P. d. Jong and J. H. Bitter, *Carbon*, 2008, **46**, 138-148.
38. K. Gong, F. Du, Z. Xia, M. Durstock and L. Dai, *Science*, 2009, **323**, 760-764.
39. S. Maldonado, S. Morin and K. J. Stevenson, *Carbon*, 2006, **44**, 1429-1437.
40. J. D. Wiggins-Camacho and K. J. Stevenson, *J. Phys. Chem. C*, 2011, **115**, 20002-20010.
41. J.-P. Tessonnier, M. Becker, W. Xia, F. Girgsdies, R. Blume, L. Yao, D. S. Su, M. Muhler and R. Schloegl, *ChemCatChem*, 2010, **2**, 1559-1561.
42. A. Rinaldi, B. Frank, D. S. Su, S. B. A. Hamid and R. Schlögl, *Chem. Mater.*, 2011, **23**, 926-928.
43. B. Mei, M. D. Sanchez, T. Reinecke, S. Kaluza, W. Xia and M. Muhler, *J. Mater Chem.*, 2011, **21**, 11781-11790.
44. E. Ventosa, W. Xia, S. Klink, F. L. Mantia, B. Mei, M. Muhler and W. Schuhmann, *Chem. Eur. J.*, 2013, **19**, 14194–14199.

45. M. Pang, C. Liu, W. Xia, M. Muhler and C. Liang, *Green Chem.*, 2012, **14**, 1272-1276.
46. T. Cotter, B. Frank, W. Zhang, R. Schlögl and A. Trunschke, *Chem. Mater.*, 2013, **25**, 3124-3136.
47. M. L. Toebes, E. M. P. van Heeswijk, J. H. Bitter, A. J. van Dillen and K. P. de Jong, *Carbon*, 2004, **42**, 307-315.
48. P. V. Lakshminarayanan, H. Toghiani and C. U. P. Jr, *Carbon*, 2004, **42**, 2433–2442.
49. K. L. Klein, A. V. Melechko, T. E. McKnight, S. T. Retterer, P. D. Rack, J. D. Fowlkes, D. C. Joy and M. L. Simpson, *J. Appl. Phys.*, 2008, **103**, 061301.
50. J. L. Figueiredo, M. F. R. Pereira, M. M. A. Freitas and J. J. M. Órfão, *Carbon*, 1999, **37**, 1379-1389.
51. A. E. Aksoylu, M. M. A. Freitas and J. L. Figueiredo, *Appl. Catal. A*, 2000, **192**, 29-42.
52. S. Kundu, Y. Wang, W. Xia and M. Muhler, *J. Phys. Chem. C*, 2008, **112**, 16869-16878.
53. W. Xia, Y. Wang, R. Bergstraesser, S. Kundu and M. Muhler, *Appl. Surf. Sci.*, 2007, **254**, 247-250.
54. W. Xia, C. Jin, S. Kundu and M. Muhler, *Carbon*, 2009, **47**, 919-922.
55. S. Kundu, W. Xia, W. Busser, M. Becker, D. A. Schmidt, M. Havenith and M. Muhler, *Phys. Chem. Chem. Phys.*, 2010, **12**, 4351-4359.
56. Y. Wang, X. Wang and M. Antonietti, *Angew. Chem. Int. Ed.*, 2012, **51**, 68-89.
57. J.-P. Tessonnier, D. Rosenthal, F. Girgsdies, J. Amadou, D. Begin, C. Pham-Huu, D. Sheng Su and R. Schlogl, *Chem. Commun.*, 2009, 7158-7160.
58. W. Xia, V. Hagen, S. Kundu, Y. Wang, C. Somsen, G. Eggeler, G. Sun, G. Grundmeier, M. Stratmann and M. Muhler, *Adv. Mater.*, 2007, **19**, 3648-3652.
59. W. Xia, X. Yin, S. Kundu, M. Sanchez, A. Birkner, C. Woll and M. Muhler, *Carbon*, 2011, **49**, 299-305.
60. A. Zhao, J. Masa, W. Schuhmann and W. Xia, *J. Phys. Chem. C*, 2013, **117**, 24283-24291.
61. W. Xia, J. Masa, M. Bron, W. Schuhmann and M. Muhler, *Electrochem. Commun.*, 2011, **13**, 593-596.
62. E. N. Nxumalo and N. J. Coville, *Materials*, 2010, **3**, 2141-2171.
63. R. Kurt and A. Karim, *ChemPhysChem*, 2001, **2**, 388-392.
64. G. S. Szymański, T. Grzybek and H. Papp, *Catal. Today*, 2004, **90**, 51-59.
65. H. Liu, Y. Zhang, R. Li, X. Sun and H. Abou-Rachid, *J. Nanopart. Res.*, 2012, **14**, 8.
66. S. Kundu, T. C. Nagaiah, W. Xia, Y. Wang, S. Van Dommele, J. H. Bitter, M. Santa, G. Grundmeier, M. Bron, W. Schuhmann and M. Muhler, *J. Phys. Chem. C*, 2009, **113**, 14302-14310.
67. A. Zhao, J. Masa, M. Muhler, W. Schuhmann and W. Xia, *Electrochimica Acta*, 2013, **98**, 139-145.
68. M. J. Becker, W. Xia, J.-P. Tessonnier, R. Blume, L. Yao, R. Schloegl and M. Muhler, *Carbon*, 2011, **49**, 5253-5264.
69. S. van Dommele, A. Romero-Izquirdo, R. Brydson, K. P. de Jong and J. H. Bitter, *Carbon*, 2008, **46**, 138-148.
70. J. L. Lyon and K. J. Stevenson, *Langmuir*, 2007, **23**, 11311-11318.
71. J. Masa, A. Zhao, W. Xia, M. Muhler and W. Schuhmann, *Electrochimica Acta*, 2014, **128**, 271-278.
72. C. Jin, W. Xia, P. Chen and M. Muhler, *Catal. Today*, 2012, **186**, 128-133.
73. J. Masa, A. Zhao, W. Xia, Z. Sun, B. Mei, M. Muhler and W. Schuhmann, *Electrochem. Commun.*, 2013, **34**, 113-116.
74. J. Zhang, M. Comotti, F. Schuth, R. Schlogl and D. S. Su, *Chem. Commun.*, 2007, 1916-1918.
75. T. Osaki and T. Mori, *React Kinet. Catal. Lett.*, 2006, **89**, 333-339.
76. H. Ohme and T. Suzuki, *Energy & Fuels*, 1996, **10**, 980-987.
77. L. Dai, Y. Xue, L. Qu, H.-J. Choi and J.-B. Baek, *Chem. Rev.*, 2015, **115**, 4823–4892.
78. B. Šljukić, C. E. Banks and R. G. Compton, *Nano Lett.*, 2006, **6**, 1556-1558.
79. C. E. Banks, A. Crossley, C. Salter, S. J. Wilkins and R. G. Compton, *Angew. Chem. Int. Ed.*, 2006, **45**, 2533-2537.
80. S. Kattel, P. Atanassov and B. Kiefer, *Phys. Chem. Chem. Phys.*, 2013, **15**, 148-153.
81. A. Zhao, J. Masa, W. Xia, A. Maljusch, M.-G. Willinger, G. Clavel, K. Xie, R. Schlögl, W. Schuhmann and M. Muhler, *J. Am. Chem. Soc.*, 2014, **136**, 7551-7554.
82. M. L. Toebes, J. A. van Dillen and K. P. de Jong, *J. Molecular Catal. A*, 2001, **173**, 75-98.
83. F. Coloma, A. Sepulveda-Escribano, J. L. G. Fierro and F. Rodriguez-Reinoso, *Langmuir*, 1994, **10**, 750-755.
84. Y. F. Yang, L. T. Jia, B. Hou, D. B. Li, J. G. Wang and Y. H. Sun, *J. Phys. Chem. C*, 2014, **118**, 268-277.
85. H. Xiong, M. A. Motchelaho, M. Moyo, L. L. Jewell and N. J. Coville, *Appl Catal A*, 2014, **482**, 377-386.
86. L. M. Chew, P. Kangvansura, H. Ruland, H. J. Schulte, C. Somsen, W. Xia, G. Eggeler, A. Worayingyong and M. Muhler, *Appl. Catal. A*, 2014, **482**, 163-170.
87. Y. Cheng, C. W. Xu, P. K. Shen and S. P. Jiang, *Appl. Catal. B.*, 2014, **158**, 140-149.
88. B. S. Zhang, L. D. Shao, W. Zhang, X. Y. Sun, X. L. Pan and D. S. Su, *ChemCatChem*, 2014, **6**, 2607-2612.
89. L. Zhang, G. Wen, H. Liu, N. Wang and D. S. Su, *ChemCatChem*, 2014, **6**, 2600-2606.
90. S. Abate, M. Freni, R. Arrigo, M. E. Schuster, S. Perathoner and G. Centi, *ChemCatChem*, 2013, **5**, 1899-1905.
91. H. Liu, L. Zhang, N. Wang and D. S. Su, *Angew. Chem. Int. Ed.*, 2014, **53**, 12634-12638.
92. R. Arrigo, M. E. Schuster, S. Abate, S. Wrabetz, K. Amakawa, D. Teschner, M. Freni, G. Centi, S. Perathoner, M. Hävecker and R. Schlögl, *ChemSusChem*, 2014, **7**, 179-194.
93. P. D. Burton, T. J. Boyle and A. K. Datye, *J. Catal.*, 2011, **280**, 145-149.
94. P. R. Chen, L. M. Chew, A. Kostka, M. Muhler and W. Xia, *Catal. Sci. Technol.*, 2013, **3**, 1964-1971.
95. R. Chetty, W. Xia, S. Kundu, M. Bron, T. Reinecke, W. Schuhmann and M. Muhler, *Langmuir*, 2009, **25**, 3853-3860.
96. P. Chen, L. M. Chew and W. Xia, *J. Catal.*, 2013, **307**, 84-93.
97. M. Sanchez, P. Chen, T. Reinecke, M. Muhler and W. Xia, *ChemCatChem*, 2012, **4**, 1997-2004.
98. C.-T. Wang, H.-Y. Chen and Y.-C. Chen, *Sensors and Actuators B-Chemical*, 2013, **176**, 945-951.
99. S. Ordóñez, E. Díaz, R. F. Bueres, E. Asedegbega-Nieto and H. Sastre, *J. Catal.*, 2010, **272**, 158-168.
100. R. W. Gosselink, W. Xia, M. Muhler, K. P. de Jong and J. H. Bitter, *ACS Catal.*, 2013, **3**, 2397-2402.
101. R. W. Gosselink, R. van den Berg, W. Xia, M. Muhler, K. P. de Jong and J. H. Bitter, *Carbon*, 2012, **50**, 4424-4431.
102. M. Brun, Berthet, A., Bertolini, J.C., *J. Electron Spectroscopy and Related Phenomena*, 1999, **104**, 55-60.
103. S. Biniak, R. Diduszko, W. Gac, M. Pakuła and A. Świątkowski, *Reac. Kinet. Mech. Cat.*, 2010, **101**, 331-342.
104. H. R. Byon, J. Suntivich and Y. Shao-Horn, *Chem. Mater.*, 2011, **23**, 3421-3428.
105. M. Yuasa, A. Yamaguchi, H. Itsuki, K. Tanaka, M. Yamamoto and K. Oyaizu, *Chem. Mater.*, 2005, **17**, 4278-4281.
106. J. Masa, T. Schilling, M. Bron and W. Schuhmann, *Electrochimica Acta*, 2012, **60**, 410-418.
107. Z. Shi, H. Liu, K. Lee, E. Dy, J. Chlistunoff, M. Blair, P. Zelenay, J. Zhang and Z.-S. Liu, *J. Phys. Chem. C*, 2011, **115**, 16672-16680.

Graphical and textual abstract

Surface functionalities and defects strongly influence the interactions between metal species and nitrogen-functionalized carbon nanotubes.